

Cite this: *RSC Adv.*, 2017, 7, 41970Received 3rd May 2017  
Accepted 16th August 2017

DOI: 10.1039/c7ra04979j

rsc.li/rsc-advances

# Influence of HDI as a cathode film-forming additive on the performance of $\text{LiFe}_{0.2}\text{Mn}_{0.8}\text{PO}_4/\text{C}$ cathode†

Xiaoyue Xu,<sup>b</sup> Yinping Qin,<sup>b</sup> Wenchao Yang,<sup>b</sup> Dandan Sun,<sup>a</sup> Yang Liu,<sup>ID</sup>\*<sup>a</sup>  
Bingkun Guo<sup>a</sup> and Deyu Wang<sup>\*b</sup>

Herein, we construct a polymer protective layer on  $\text{LiFe}_{0.2}\text{Mn}_{0.8}\text{PO}_4/\text{C}$  particles with hexamethylene diisocyanate *via* the onium ionization–polymerization reaction. This membrane obviously improves  $\text{LiFe}_{0.2}\text{Mn}_{0.8}\text{PO}_4/\text{C}$ 's rate capability and cyclic stability. It exerts a more significant effect on samples with less carbon, demonstrating its function to ameliorate the conductive network.

## Introduction

Lithium ion batteries (LIBs) have been widely utilized in the markets of commercial electronics, vehicles and smart grids due to their excellent comprehensive performance.<sup>1,2</sup> Similar to other systems, LIB behaviour is highly dependent on its interfacial stability, particularly with regard to cyclic and rate capability.<sup>3,4</sup> In contrast to the series of progress on improving the quality of the graphite/electrolyte interface,<sup>5</sup> the similar studies on cathodes were highly absent in the community.<sup>6</sup>

In our previous work, we developed a new method to construct a polymer membrane on ternary layer oxides.<sup>7</sup> This membrane significantly improved the electrochemical performance of  $\text{LiNi}_{1/3}\text{Co}_{1/3}\text{Mn}_{1/3}\text{O}_2$  cathode with the appropriate amount of hexamethylene diisocyanate (HDI), which enhanced the interfacial electronic conductivity to  $\sim 1 \text{ k}\Omega$ , *i.e.*  $\sim 7$  orders higher than that of  $\text{LiNi}_{1/3}\text{Co}_{1/3}\text{Mn}_{1/3}\text{O}_2$ . Therefore, we hypothesized that the addition of HDI may facilitate the electron's transportation for other cathodes, particularly for insulated cathodes.

Lithium manganese iron phosphate-based material is a type of promising novel cathode with electronic conductivity of  $< 10^{-10} \text{ S cm}^{-1}$ .<sup>8–10</sup> It is possible to replace the widely used lithium iron phosphate due to its higher redox potential, resulting in  $\sim 15\%$  extra energy density.<sup>11–13</sup> Owing to its much lower electronic conductivity compared to that of  $\text{LiFePO}_4$ , its particles should be diminished to  $\sim 100 \text{ nm}$  to ensure acceptable performance,<sup>14,15</sup> and a large amount of carbon was utilized to sustain the good electronic transportation.<sup>16–18</sup> Because the cutoff potential of lithium manganese phosphate ( $\sim 4.4 \text{ V vs. Li}^+/\text{Li}$ ) is higher than the decomposing potential of PC ( $\sim 4.3 \text{ V vs. Li}^+/\text{Li}$ ),<sup>19,20</sup> a similar polymer layer as we reported<sup>7</sup> is probably

built on the surface of phosphate materials, which may benefit the cathodes' electrochemical performance.

In this study, we construct a polymer membrane on  $\text{LiMn}_{0.8}\text{Fe}_{0.2}\text{PO}_4/\text{C}$  with hexamethylene diisocyanate and investigate its influence on the phosphate cathode materials. HDI is polymerized with the oxidative species of propylene carbonate to produce the amide-containing membrane. This protective layer could repair the flaws of C-coating film to improve the cathode performances in cycling and rating.

## Results and discussion

The prepared  $\text{LiFe}_{0.2}\text{Mn}_{0.8}\text{PO}_4/\text{C}$  materials were tested by XRD, TEM and SEM. In Fig. S1,† all the XRD patterns are identified as the pure phase of crystalline olivine of  $\text{LiFe}_{0.2}\text{Mn}_{0.8}\text{PO}_4/\text{C}$ , as reported previously.<sup>21</sup> TEM and SEM images of  $\text{LiFe}_{0.2}\text{Mn}_{0.8}\text{PO}_4/\text{C}$  with 2 wt% C-coating are presented as a typical sample (Fig. S2 and S3†). The particles are  $\sim 100 \text{ nm}$ , with the morphology of coral shapes, as shown in 1b and c. The carbon coating contents after the calcination are 1.4 wt%, 2.0 wt%, 3.6 wt% and 6.8 wt% as confirmed by a high frequency infrared carbon sulfur analyzer (CS844).

The film forming characteristics were investigated in an electrolyte containing 500 mM HDI. 2 wt% carbon coating  $\text{LiFe}_{0.2}\text{Mn}_{0.8}\text{PO}_4/\text{C}$  was selected as the cathode sample. As shown in Fig. 1 and S2,† in contrast to the almost intact morphology of  $\text{LiFe}_{0.2}\text{Mn}_{0.8}\text{PO}_4/\text{C}$  after polarization, a new layer with 2.6–3 nm thickness is observed on the particle surface. It also repairs the flaws of the carbon layer and even directly grows on the phosphate surface. The SEM images (Fig. 1c and d) show similar characteristics. After being charged for 3 hours, the edges of cathode grains in the base electrolyte are clear-cut, and particles are conglomerated when 500 mM HDI was added. All the morphology images confirm that a surface layer is automatically built on the surface of carbon or  $\text{LiFe}_{0.2}\text{Mn}_{0.8}\text{PO}_4$ .

X-ray photoelectron spectroscopy measurements were performed to identify the constitution of the surface layer on the

<sup>a</sup>Materials Genome Institute, Shanghai University, Shanghai, 200444, China. E-mail: liuyang81@shu.edu.cn

<sup>b</sup>Ningbo Institute of Materials Technology and Engineering, Chinese Academy of Sciences, Ningbo, 315201, China. E-mail: wangdy@nimte.ac.cn

† Electronic supplementary information (ESI) available. See DOI: 10.1039/c7ra04979j



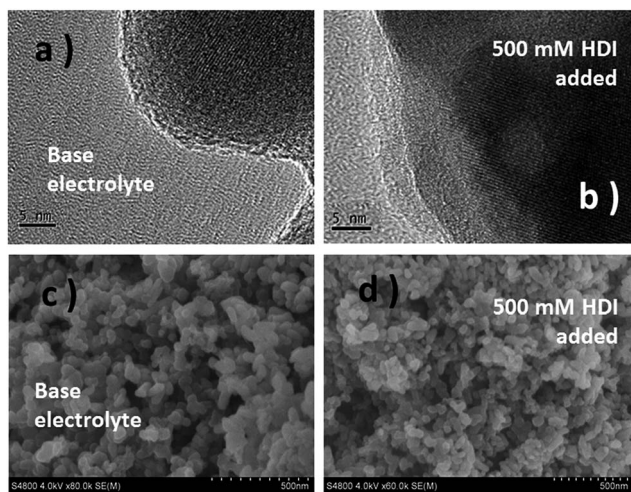


Fig. 1 TEM (a and b) and SEM (c and d) images of electrodes in the base and HDI-added electrolytes charged at 4.4 V (vs.  $\text{Li}^+/\text{Li}$ ) for 3 hours.

sample. The peak at 401 eV in the N 1s XPS spectra (Fig. 2a) is consistent with the amide group in our previous work,<sup>7</sup> indicating that the onium ionization–polymerization reaction was performed. It could be inferred that an amide-based polymer layer is formed on the surface of  $\text{LiFe}_{0.2}\text{Mn}_{0.8}\text{PO}_4/\text{C}$ .

The electrochemical influence of this membrane was evaluated *via* cyclic voltammetry. The electrolyte containing 10 mM HDI was used as the standard. The sample shows a lower start-up oxidative potential and 36.5% higher electron quantity in the system with HDI compared to those of the pristine system (Fig. 2b). The improvements on the electrochemical performance of  $\text{LiFe}_{0.2}\text{Mn}_{0.8}\text{PO}_4/\text{C}$  prove the positive effects of the HDI-built-layer on the phosphate material.

The influence of this membrane was further investigated for the samples with different carbon coating amount *via* electrochemical impedance spectroscopy. The electrolytes without and with 10 mM HDI were compared. As shown in Fig. 2c and d, the first semicircle is ascribed to the surface film resistance of the cell ( $R_{\text{ct}}$ ), and the second is attributed to the charge-transfer resistance of cell ( $R_{\text{e}}$ ). In base electrolyte, the interfacial impedances decrease for the samples of C-coating from 1.4 wt% to 3.6 wt% and increase from 3.6 wt% to 6.8 wt%. When 10 mM HDI was added, all the interfacial impedances are similar and decreased compared to the base samples (Table S1†). These results prove that the surface films formed by HDI-PC diminish the interfacial impedances on the electrodes, which is beneficial for electron's transportation.

The influence of this protective polymer membrane on the electrochemical performance of  $\text{LiFe}_{0.2}\text{Mn}_{0.8}\text{PO}_4/\text{C}$  was investigated with different carbon contents in Fig. 3. The potential differences between charge and discharge curves at 0.5C in Fig. 3a and b reflect polarization, which is related to the interfacial conductance between  $\text{LiFe}_{0.2}\text{Mn}_{0.8}\text{PO}_4/\text{C}$  cathodes and electrolytes. The lift of discharging platform potentials should be considered as the lower interfacial resistance slumped by the *in situ*-formed film in the first charging process. All samples

deliver better cycling performances with HDI than those without additive. The samples with 2% carbon and higher ratio remain at  $\sim 98\%$  of the initial capacity at the 500th cycle (Fig. 3c and d), 0.5C. For the 1.4 wt% carbon coating sample with HDI, although its capacity was seriously faded, its initial discharge capacity is improved from  $74.4 \text{ mA h g}^{-1}$  to  $149.5 \text{ mA h g}^{-1}$  by this membrane and still maintains  $50.7 \text{ mA h g}^{-1}$ , 2 times higher than the system without HDI, at the 500th cycle. These results demonstrate that our interface design facilitates the carriers' transportation of  $\text{LiFe}_{0.2}\text{Mn}_{0.8}\text{PO}_4/\text{C}$ . Combining pure  $\text{LiMn}_{0.8}\text{Fe}_{0.2}\text{PO}_4$  shows little discharge capacities in the base and HDI-added electrolytes (Fig. S4†); the fast capacity fading of the sample with 1.4 wt% C-coating may suggest that less C-coating leads to a stable interfacial layer that cannot be built on the cathode surface even if HDI is added.

Comparison of the rate capability of the films in  $\text{Li}/\text{LiFe}_{0.2}\text{Mn}_{0.8}\text{PO}_4/\text{C}$  cells is shown in Fig. 3e and f. With 10 mM HDI added, the cells with different C-coatings deliver more discharge capacities at varied current densities. When the additive was added, the cell with 2.0 wt% C-coating displays the best rate capability. At a current density of 0.1C, the cell presents an initial discharge capacity of  $163.2 \text{ mA h g}^{-1}$  and retains  $100.6 \text{ mA h g}^{-1}$  at 10C, whereas the cell with 2.0 wt% C-coating in the base electrolyte is  $58.1 \text{ mA h g}^{-1}$  at 10C; the cell with 6.8 wt% C-coating is  $80.8 \text{ mA h g}^{-1}$ . When the rate returns to 0.5C, all the discharge capacities are recovered. At 10C, the trend of the discharge capabilities of cells with base electrolyte only is similar to the quantity of C-coatings. With HDI added, all of the samples show better capacities. It may be a mere coincidence that in cycling and rating, the capacity differences are similar, whereas the same electrodes in base electrolyte and HDI are added (Fig. 3g and h), but the changes in trend of capacity differences with C-coating show that the film building strategy enhances discharge performances of the phosphate material batteries between 0.1C and

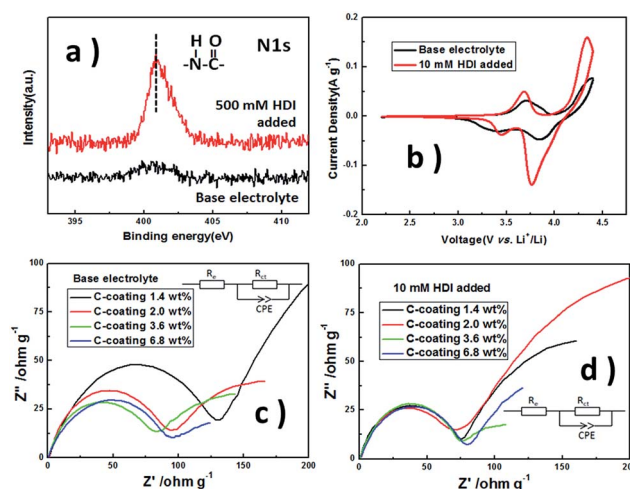


Fig. 2 XPS (a) and CV (b) spectra of  $\text{LiFe}_{0.2}\text{Mn}_{0.8}\text{PO}_4/\text{C}$  (2.0 wt%) cathodes in different electrolytes charged at 4.4 V (vs.  $\text{Li}^+/\text{Li}$ ) for 3 hours, scanned with  $0.1 \text{ mV s}^{-1}$ . EIS of  $\text{Li}/\text{LiFe}_{0.2}\text{Mn}_{0.8}\text{PO}_4/\text{C}$  cells with different C-coatings in base (c) and 10 mM HDI added (d) electrolytes charged at 4.4 V (vs.  $\text{Li}^+/\text{Li}$ ) for 3 hours. The inset images are the simulated models.



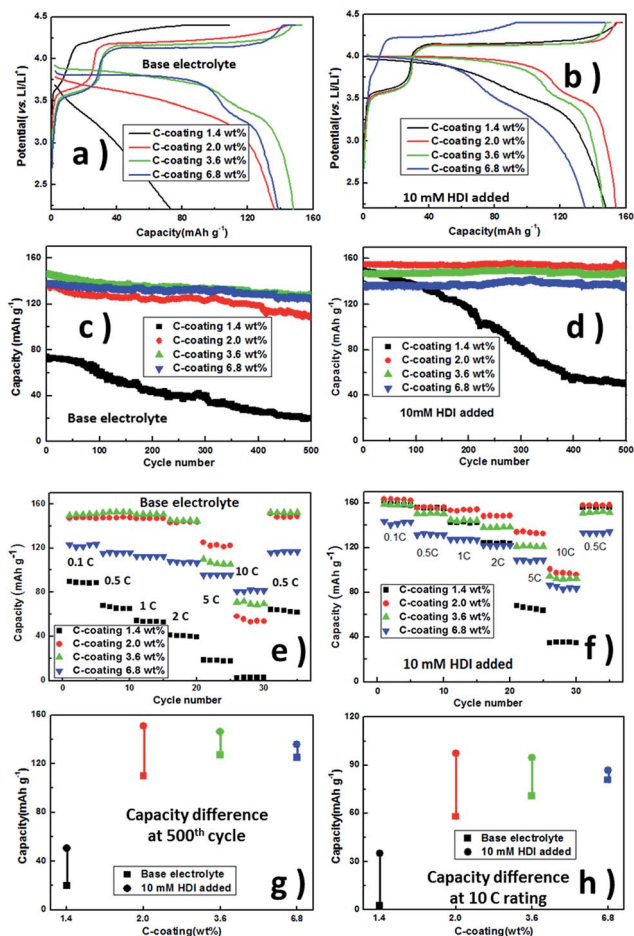


Fig. 3 The first charge–discharge curves (a and b), cycling (c and d) and rating (e and f) performances of Li/LiFe<sub>0.2</sub>Mn<sub>0.8</sub>PO<sub>4</sub>/C cells with different C-coatings in base and 10 mM HDI added electrolytes at RT, and the capacity difference (g and h) between cells with and without HDI added at the 500th cycle and 10C rating.

10C. As suggested above, appropriate C-coating makes the discharge capacity and capacity retention of LiMn<sub>0.8</sub>Fe<sub>0.2</sub>PO<sub>4</sub> acceptable, and the HDI-formed layer could further improve the initial capacities, capacity retentions and high rate capabilities of samples with 1.4–3.6 wt% C-coating.

## Conclusions

In summary, a polymer interfacial layer has been built successfully on the surface of LiFe<sub>0.2</sub>Mn<sub>0.8</sub>PO<sub>4</sub>/C based on an onium ionization–polymerization reaction. The layer improved the electrochemical performance of LiFe<sub>0.2</sub>Mn<sub>0.8</sub>PO<sub>4</sub>/C composites and diminished the influence of carbon contents. Among the investigated systems, the samples with 2.0 wt% carbon and 10 mM HDI electrolyte presented the best performance, delivering 163.2 mA h g<sup>−1</sup> at 0.1C and 100.6 mA h g<sup>−1</sup> at 10C, and maintaining ~98% after 500 cycles at 0.5C. The results confirm that the onium ionization–polymerization reaction-based design strategy could be applied to phosphate and cathodes with C-coating.

## Conflicts of interest

There are no conflicts to declare.

## Acknowledgements

This study was supported by the National Natural Science Foundation of China (Grant No. 21503247, 51572273) and the Ningbo Natural Science Foundation (Grant No. 2015A610250).

## References

- 1 K. Xu, *Chem. Rev.*, 2004, **104**, 4303–4418.
- 2 J. B. Goodenough and Y. Kim, *Chem. Mater.*, 2010, **22**, 587–603.
- 3 S. Phul, A. Deshpande and B. Krishnamurthy, *Electrochim. Acta*, 2015, **164**, 281–287.
- 4 V. A. Agubra and J. W. Fergus, *J. Power Sources*, 2014, **268**, 153–162.
- 5 S. J. An, J. L. Li, C. Daniel, D. Mohanty, S. Nagpure and D. L. Wood III, *Carbon*, 2016, **105**, 52–76.
- 6 K. Xu, *Chem. Rev.*, 2014, **114**, 11503–11618.
- 7 Y. Liu, Y. Qin, Z. Peng, J. J. Zhou, C. J. Wan and D. Y. Wang, *J. Mater. Chem. A*, 2015, **3**, 8246–8249.
- 8 M. Köntje, M. Memm, P. Axmann and M. Wohlfahrt-Mehrens, *Prog. Solid State Chem.*, 2014, **42**, 106–117.
- 9 S.-M. Oh, S.-W. Oh, C.-S. Yoon, B. Scrosati, K. Amine and Y.-K. Suni, *Adv. Funct. Mater.*, 2010, **20**, 3260–3265.
- 10 J. Wolfenstine, U. Lee, B. Poesse and J. L. Allen, *J. Power Sources*, 2005, **144**, 226–230.
- 11 L. Dimesso, C. Förster, W. Jaegermann, J. P. Khanderi, H. Tempel, A. Popp, J. Engstler, J. J. Schneider, A. Sarapulova, D. Mikhailova, L. A. Schmitt, S. Oswald and H. Ehrenberg, *Chem. Soc. Rev.*, 2012, **41**, 5068–5080.
- 12 F. Pan, W.-l. Wang, D. Chen and W. Yan, *J. Mater. Chem.*, 2011, **21**, 14680–14684.
- 13 V. Aravindan, J. Gnanaraj, Y.-S. Lee and S. Madhav, *J. Mater. Chem. A*, 2013, **1**, 3518–3539.
- 14 A. Yamada, M. Hosoya, S.-C. Chung, Y. Kudo, K. Hinokuma, K.-Y. Liu and Y. Nishi, *J. Power Sources*, 2003, **119**, 232–238.
- 15 B. Zhang, X. J. Wang, Z. J. Liu, H. Li and X. J. Huang, *J. Electrochem. Soc.*, 2010, **157**, A285–A288.
- 16 C. L. Wei, W. He, X. D. Zhang, J. X. Shen and J. Y. Ma, *New J. Chem.*, 2016, **40**, 2984–2999.
- 17 D. Tao, S. P. Wang, Y. C. Liu, Y. Dai, J. X. Yu and X. R. Lei, *Ionics*, 2015, **21**, 1201–1239.
- 18 F. X. Mao, W. Guo and J. M. Ma, *RSC Adv.*, 2015, **5**, 105248–105258.
- 19 K. Kanamura, S. Toriyama, S. Shiraishi and Z. Takehara, *J. Electrochem. Soc.*, 1995, **142**, 1383–1389.
- 20 S. Matsuta, Y. Kato, T. Ota, H. Kurokawa, S. Yoshimura and S. Fujitani, *J. Electrochem. Soc.*, 2001, **148**, A7–A10.
- 21 X. Y. Xu, T. Wang, Y. J. Bi, M. Liu, W. C. Yang, Z. Peng and D. Y. Wang, *J. Power Sources*, 2017, **341**, 175–182.

